Fachtagung "Experimentelle Strömungsmechanik"
6.–8. September 2022, Ilmenau

Neutronenradiographie des anisotropen Drainageflusses

Neutron radiography of the anisotropic drainage flow

Artem Skrypnik[1], Pavel Trtik[2], Katie Cole[3], Tobias Lappan[4], Pablo R. Brito-Parada[5], Stephen J. Neethling[5], Kerstin Eckert[1,4], and Sascha Heitkam[1,4]
[1]Institute of Process Engineering and Environmental Technology, TU Dresden, Dresden, Germany
[2]Laboratory for Neutron Scattering and Imaging, Paul Scherrer Institut, Switzerland
[3]Department of Physics, University of Cape Town, South Africa
[4]Institute of Fluid Dynamics, Helmholtz-Zentrum Dresden-Rossendorf, Germany
[5]Department of Earth Science and Engineering, Imperial College London, UK

Schaumdrainage, Drainage Anisotropie, Neutronenradiographie
Foam drainage, dranage anisotropie, neutron radiography

Abstract

Liquid drainage through the foam is driven by gravity, capillary, and to a lesser extent, viscous forces. If the foam is free of stress, the liquid distributes uniformly. The imposed stress changes the alignment of foam's structural elements. Preceding numerical simulations predicted that a vertical drainage flow will be deflected horizontally if the foam is sheared. We investigated such phenomena by measuring the liquid fraction distribution within the foam. A foam in a flat rectangular cell was subjected to shear stress under a forced liquid supply at the top of the cell. 2D neutron radiography images of stress-free and sheared foam were analyzed. Deflections of the drainage fronts were detected, which then were correlated with the foam shearing magnitude. To the best of our knowledge, this is the first experimental observation of anisotropic drainage in a liquid foam.

Introduction

Liquid foam is a heterogeneous media with distinctive rheological properties (Doller & Raufaste, 2014, Höhler & Cohen-Addad 2005). It consists of gaseous bubbles distributed in a liquid media. The liquid is held within interstitial channels (known as Plateau borders) and liquid films between the neighbouring bubbles. Under the influence of gravity and counteraction by capillary and viscous forces, the liquid distributes within the foam, considerably affecting the foam structural and rheological properties. Liquid transport through the foam, or drainage (Princen 1990), is a complex process, which is affected by the chemical composition of the foaming solution, the surface mobility, bubble size distribution and many other factors (saint-James 2006, Safouane et al. 2001, Koehler S. et. al. 2000). A conventional approach to determine the liquid distribution in a foam is to solve the drainage equation (Verbist et al. 1996, Koehler et al. 2000, Huzler et al. 2005). This requires known geometrical parameters of the foam, physicochemical properties of the solution and assumed mobility of the interfaces leading to vertex or Plateau border dissipation (Huzler et al. 2005, Koehler et al. 1999, Koehler et al. 2000). The solution of the corresponding equation will yield the tem-

GALA e.V., Karlsruhe, Germany, ISBN 978-3-9816764-8-8

porary and spatial evolution of liquid fraction $\varphi_l = V_l/V_f$, i.e. the ratio of liquid volume V_l to total foam volume V_f.
The drainage equation assumes foam to be isotropic, meaning uniform properties in any direction. However, in a length scale of a single Plateau border (Koehler et al. 2004, Cohen-Addad et al. 2015) it might be more complex. For instance, contribution of the liquid transport through the liquid films (Carrier et al. 2002, Koehler et al. 2004) is still debated. Drainage anisotropy in the foam has also been reported. Carrier et al. (Carrier, Colin 2002) related the anisotropy to the difference of a film thickness according to its spatial orientation. Neethling (Neethling 2006) has shown the relation between the applied shearing stress to the foam and the horizontal deflection of a vertical drainage flow. The latest might induce convective rolls (Huzler et al. 2007) in a foam column, as shown in Heitkam et al. (Heitkam 2021), which, for instance, hinders a foam removal in a flotation processes.
The predictions of Neethling (Neethling 2006) were based on numerical simulation of foam structure, performed with Surface Evolver software (Brakke 1992), and up to date there is no experimental proof of the predicted phenomena. We aim to provide experimental evidence of the effect of a simple shear on the drainage anisotropy in a liquid foam. We organize the paper as follows: first, the details on the experimental installation and utilized measurement techniques are provided. Then, we present the results of a liquid fraction measurements within the foam domain. This, distribution, then related to a drainage front position. Finally, in a discussion section, we characterize the observed phenomena and its consequence.

Materials and methods

Experimental setup

The experimental investigation focused on qualitative observation of liquid distribution within the sheared and non-sheared foam. The experimental setup with its components' arrangement is shown in Figure 1 (a, b). The measurement installation includes a neutron beam source, which path is aligned and parallelized by the collimator, a foam cell placed in a beam path, and the image acquisition system of scintillator, mirror and CCD camera (Fig. 1, a). The foam was generated in a 3D printed rectangle cell (width 400 mm) which includes 5 mm thick glass plates of width 400 mm, separated by the distance of 100 mm. A foaming solution of water and dissolved sodium dodecyl sulfate (SDS, 6 g/l) was poured in the foam cell, providing the liquid filling level of $h_{solution} \approx 67$ mm.

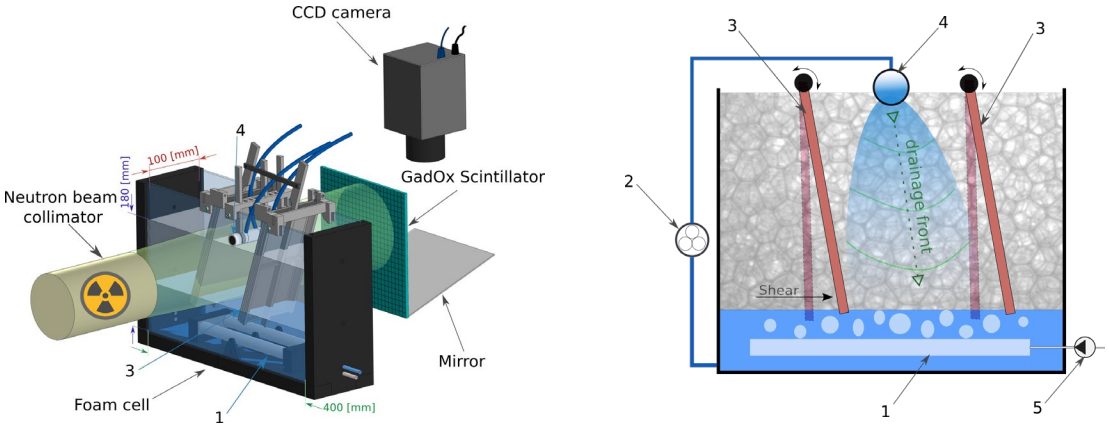

(a) (b)

Figure 1: The arrangement of the measurement setup (a) and the scheme of the cell with its component parts: 1. the bubble generator; 2. the peristatic pump; 3. shearing plates; 4. the drainage liquid source; 5.the air pump.

GALA e.V., Karlsruhe, Germany, ISBN 978-3-9816764-8-8

The foam has been produced by pumping air with trace of perflexane C_6F_{14} through a porous or orificed tube, which was submerged in a foaming solution and fixed at the bottom of the cell. The airflow rate $\dot{Q_{air}}$ was kept constant by a diaphragm vacuum pump (Laboport N 86 KN.18), and was equal to 6.0 l/min. We varied the bubble size by utilizing two different high-density polyethylene porous tubes, with pore sizes of 100 and 250 µm, and a tube with uniformly spaced orifices of d_0 = 0.8 mm.
The average bubble diameters < D > and their related statistical parameters were evaluated by two means. Firstly, by analysis of consecutive images at the top of a bubble generator. Each bubble was approximated by an ellipse. Its estimated semi-minor axis *a* and semi-major axis *b*, and volume $V_{el} = 4/3\ \pi a b^2$, then was transferred to the equivalent diameter of a bubble $d_{eq} =< D >= \sqrt[3]{8ab^2}$ mm. Secondly, we extracted a small volume of foam from the bulk of the foam, which then was placed between two thin glass plates spaced by *z=1* (mm). The area of the squeezed bubbles Ab and its volume $V_b = A\,z$ give the equivalent bubble diameter,$< D >= d_{eq} = \sqrt[3]{6/\pi V_b}$. The standard deviation of the estimated average bubble diameter <*D*> is utilized as a measure for the bubble size polydispersity *p*. The two aforementioned methods were found to be well-aligned, and the corresponding measurement results are listed in Table 1

Table 1: The parameters of the experiments

Bubble diameter	< D >, mm	2.01	3.27	4.70
Polydispersity	p, %	20	20	10
Drainage flow rate	$\dot{q_w}$, ml/min	32	53	107

Within the scope of all experiments, we extracted surfactant solution from the bottom of the cell and constantly≈provided it at the top of the cell by means of a Watson Marlow 323 DU peristaltic pump. To ensure the uniform supply of the surfactant solution, a porous tube of $d_t = 19.7$ mm outer diameter was used as the water source. The tube was located at the center of the foam cell, filling the whole foam cell thickness, δ_c. The vertical distance between the water surface at the cell bottom and the drainage tube at its top was h_{surf}=110 mm. The corresponding drainage flow rates magnitude are listed in Table 1.
Two vertical plates were mounted perpendicular to the neutron beam path and glass walls. We generated the foam between the two plates having a distance of 100 mm. This distance was kept constant, while the plates were inclined during the experiments, yielding foam shearing. We controlled the plate displacement at the bottom of the cell, relating the shift magnitude to the value of the global stain *ε.*

Experimental setup

The foam liquid fraction *φ*, or distribution of the liquid within the cell, the pivotal parameter that we quantified with a high spatial resolution. The neutron radiographic facility NEUTRA at PSI Switzerland provides the required parameters for the quantitative assessment (Lehman et al. 2001). The measurement principle relates the transmittance of thermal neutrons through the studied object with its material composition. In the case of liquid foam, we determine the amount of water δ_w along the beam path, as the function of the incident I_0 and transmitted *I* neutron beam intensity:

$$I = I_0 exp(-\mu\delta_w) \quad (1)$$

GALA e.V., Karlsruhe, Germany, ISBN 978-3-9816764-8-8

where the parameter μ denotes the linear neutron attenuation coefficient of the corresponding material. More details on the liquid fraction determination in foams are presented in (Heitkam et al. 2018). As the foam is a two-component system, and air to a large extent is transparent to neutrons, the major contribution to the neutron attenuation is due to water. Thus, it is straightforward to determine the local liquid fraction of foam

$$\varphi = \delta_w / \delta_c$$

with the known value of liquid thickness δ_w along the beam in relation to the foam thickness δ_c.

The major issue, however, is the accurate determination of incident to transmitted beam flux ratio I/I_0. This also involves the subtraction of neutron scattering, which distorts the measurements. We adopted the approach presented in Carminati et al. (Carminati et al. 2019). The scattering contribution is estimated by the set of black bodies, equally spaced along the field of view. They are expected to be non-transparent to the neutrons and thus allow approximating the beam scattering magnitude in their shadow (Carminati et al. 2019). The beam fluxes I and I_0 were determined by relating a visible light intensity generated by the GadOx scintillator and recorded by the CCD camera (Fig. 1) for the case of the empty and foam-filled cells, respectively. The corresponding digital signal values I_0 and I were encoded as 16-bit images. A low surfactant concentration in the SDS solution allows us to assume that the foaming solution consists of pure water, with an attenuation coefficient magnitude of μ = 3.6 cm^{-1}. Thus, equation 1 provides a two-dimensional map of liquid fraction values φ of the foam cell placed in the beam path.

The foam cell was placed perpendicular to the beam path, such that neutrons transmitted the cell thickness of 100 mm between the glass plates. The field of view for the obtained image is shown in Figure 2, a. The high neutron flux allowed us to obtain the liquid fraction distribution with the spatial resolution of 0.073 mm/px, and temporary resolution up to 10 frames/sec (0.1 frames/sec has been used) The signal recorded by the camera corresponds to the number of neutrons, impinging the scintillator, and thus the camera exposure time. We set the exposure time to equal 10 sec within the scope of all the experiments, yielding the required signal magnitude. The example of the estimated liquid fraction distribution is shown in Figure 2, b.

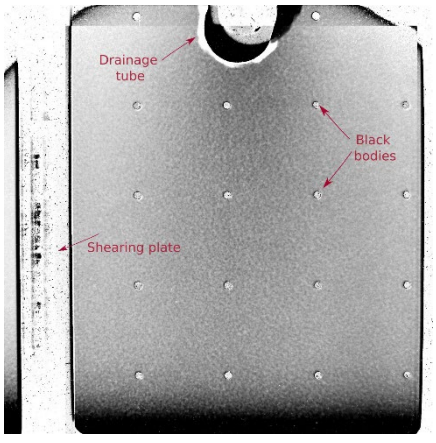

(a) (b)

Figure 2: An example of the field of view (FOV) for radiographic image (a) and estimated liquid fraction distribution map (b).

GALA e.V., Karlsruhe, Germany, ISBN 978-3-9816764-8-8

Experimental procedure

For each shear angle an individual experiment was performed, following this procedure:

1. Shearing plates were preliminary inclined providing the desired magnitude of a strain ε;
2. Fresh foam was generated, filling the inter-plate spacing. The volume of generated foam V_f provided a 8 to 10 cm foam layer on top of the cell ($V_f \approx 1800$ cm^3).
3. The plates then were sheared from left to right in the image plane (Fig. 2, a) to be perpendicular to the cell base. Thus, we imposed a strain of ε on the foam volume. The following approach prevents a possible initiation of convective rolls due to the foam shearing (Heitkam, Eckert 2021, Huzler et al. 2007) under forced drainage, and minimizes the wall effects.
4. The desired drainage flow was provided. After waiting for 2 min, the image acquisition was started. We recoded 10 images for each experimental run, providing the required statistical information and resulting in ≈ 100 s measurement time.
5. The foam was removed completely from the cell and the next shear angle was set, continuing with point 1.

Note that the foam was produced between inclined plates, which were shifted to a vertical position only after foam production. In that way, the foam was sheared but confined between vertical plates. Thus, the vertical plates did not influence the drainage flow as inclined one would have done. The expected displacement of the drainage flow corresponding to the imposed foam shear was determined by fitting the Gaussian line (shown as a dashed line in Fig. 2b) to the liquid fraction distribution along the horizontal direction downstream of the liquid point: a green line in Fig. 2, (b). The statistical noise of the data was reduced by averaging the liquid fraction over the 40 pixels up- and downstream of the line position. The peak of the Gaussian fit was the indicator of the current drainage flow position. As predicted by Neethling (Neethling 2006), an increasing shear of the foam would increase the anisotropic drainage in horizontal direction, shifting the center of the drainage flow more and more to the right side. We tested the indicated hypothesis.
The displacement of the drainage liquid distribution at i^{th} image pixel array and the strain magnitude ε is determined as:

$$\Delta x_i^{\{\varepsilon\}} = x_i - x_0$$

The relative displacement was estimated by cutting out the corresponding displacement values at zero shear:

$$\Delta_i = \Delta x_i^{\{\varepsilon\}} - \Delta x_i^{\{0\}}$$

Figure 3, (a) shows the related Gaussian fits for three lines at the middle of the cell, its corresponding relative displacement Δ_I, and the estimated relation between the measured relative displacement and applied shear for the foam with average bubble size $\langle D \rangle$= 4.7 mm, and drainage flow of $\dot{q_w}$ = 32 ml/min (Fig. 3, b).

GALA e.V., Karlsruhe, Germany, ISBN 978-3-9816764-8-8

Results

We estimated the drainage liquid distribution for each bubble generator , i.e. different average bubble sizes (Fig. 4), and different liquid fraction: solid line — 32 ml/min, dashed line — 53 ml/min, dotted line — 107 ml/min. The examination of the obtained results reveals a clear trend: the relative displacement magnitude growth with applied strain. However, the observed behavior depends on the bubble size. As the average foam bubble size decreases, the liquid front displacement shift of the drainage flow is reduced and even vanishes.
The drainage flow rate, and corresponding liquid fraction value, also affects the estimated displacement. As the liquid fraction increases, the shift of drainage flow becomes less prominent (Fig. 4).

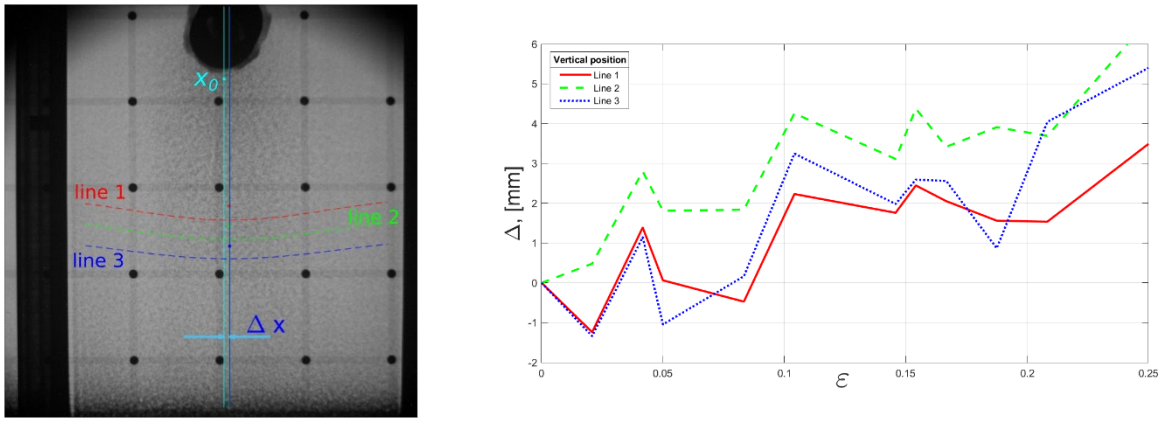

(a) (b)

Figure 3: The example of the liquid fraction displacement determination (a) and estimated displacement magnitudes (b) as the function of the applied strain ε for $< D >= 4.70$ *mm*

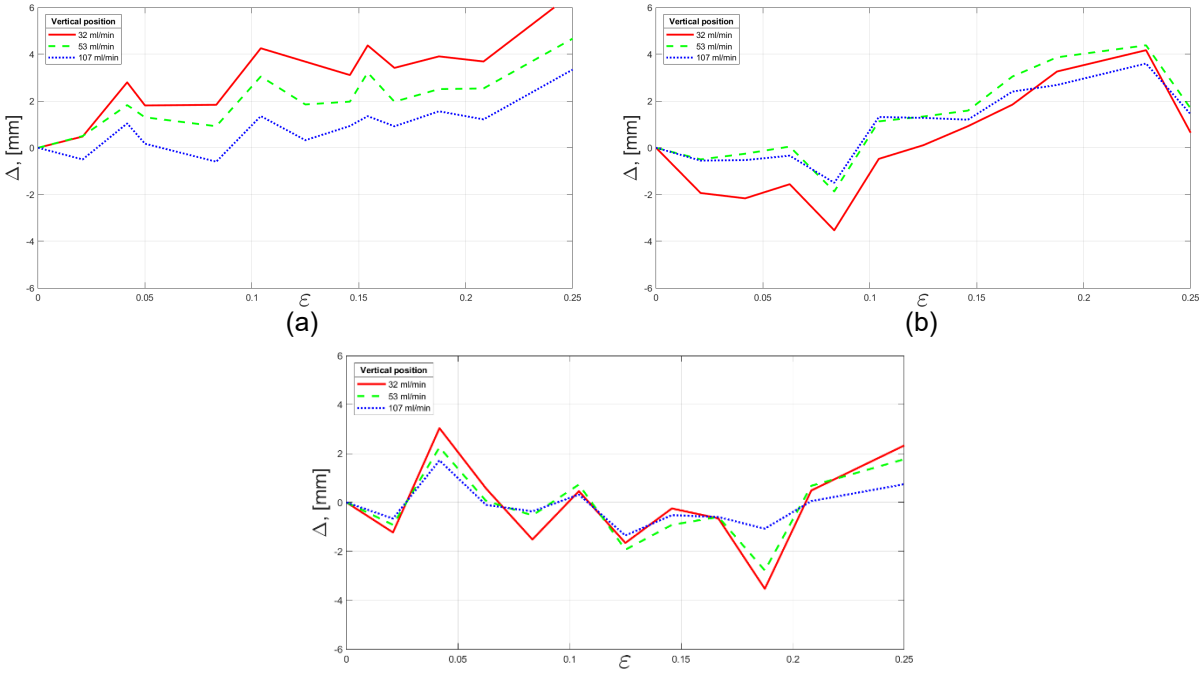

(a) (b)

(c)

Figure 4: Liquid fraction displacement as a function of applied strain: (a) <D>= 4.70 mm, (b) <*D*>= 3.27 mm, (c) <*D*>= 2.01 mm

GALA e.V., Karlsruhe, Germany, ISBN 978-3-9816764-8-8

Discussion and outlook

The magnitude of the shift of the drainage flow is significantly lower than predicted by Neethling (Neethling 2006). However, the numerical calculations were estimated for a perfectly dry, monodisperse foam. Such assumptions could not be applied to the liquid foam, utilized in the experimental measurements. As demonstrated in Figure 4, the shift of drainage is less prominent for smaller bubbles and higher liquid fractions. In these cases, the bubbles are more spherical and the Plateau borders are less prominent. Also, the yield strain reduces with increasing liquid fraction (Marze et al. 2009). Presumably, the foam was partially yielding, reducing the imposed strain angle. Moreover, even at zero imposed strain, we observed a systematic and reproducible shift of the drainage flow. This shift superimposed with the shift from the imposed strain. Potentially, within foam generation processes, some local stresses could be accumulated, for example, due to the presence of a drainage tube, or non-homogeneous bubble generation. We address this issue for the further research, where the stress and statistical strain tensors would be estimated by means of optical measurements of the Plateau border arrangement at the transparent cell wall.

Conclusion

The phenomenon of anisotropic drainage in a liquid foam was studied by means of neutron radiography. For the first time, the displacement of a drainage liquid distribution within the foam corresponding to applied shear has been observed experimentally. The impact of the strain magnitude was found to be related to the bubble size distribution and the average liquid fraction of the foam. Smaller bubbles and higher liquid fractions reduce the magnitude of anisotropic drainage.

References

Brakke K. A.: The surface evolver. Experimental Mathematics, 1(2):141–165, jan 1992. doi: 10.1080/10586458.1992.10504253.

Carminati C., Boillat P., Schmid F., Vontobel P., Hovind J., Morgano M., Siegwart R. M., Mannes D., Gruenzweig C., et al.: Implementation and assessment of the black body bias correction in quantitative neutron imaging. PLoS One, 14(1): e0210300, 2019.

Carrier V., Colin A.: Anisotropy of draining foams. Langmuir, 18(20):7564–7570, oct 2002. doi: 10.1021/la020361n.

Carrier V., Destouesse S., Colin A.: Foam drainage: a film contribution? Physical Review E, 65 (6):061404, 2002.

Cohen A., Fraysse N., Raufaste C.: Drop coalescence and liquid flow in a single plateau border. Physical Review E, 91(5):053008, 2015.

Dollet B., Raufaste C.: Rheology of aqueous foams. Comptes Rendus Physique, 15(8-9):731–747, oct 2014. doi: 10.1016/j.crhy.2014.09.008.

Heitkam S. and Eckert K.: Convective instability in sheared foam. Journal of Fluid Mechanics, 911, feb 2021. doi: 10.1017/jfm.2020.1062.

Heitkam S., Rudolph M., Lappan T., Sarma M., Eckert S., Trtik P., Lehmann E., Vontobel P., Eckert K.: Neutron imaging of froth structure and particle motion. Minerals Engineering, 119:126–129, 2018.

Höhler R., Cohen-Addad S.: Rheology of liquid foam. Journal of Physics: Condensed Matter, 17(41): R1041, 2005.

Hutzler S., Cox S. J., Janiaud E., Weaire D.: Drainage induced convection rolls in foams. Colloids and Surfaces A: Physicochemical and Engineering Aspects, 309(1-3):33–37, 2007.

Hutzler S., Cox S.J., Wang G.: Foam drainage in two dimensions. Colloids and Surfaces A: Physicochemical and Engineering Aspects, 263(1-3):178–183, aug 2005. doi: 10.1016/j.colsurfa.2005. 02.001.

Koehler S. A., Hilgenfeldt S., Stone H. A.: A generalized view of foam drainage: experiment and theory. Langmuir, 16(15):6327–6341, 2000.

GALA e.V., Karlsruhe, Germany, ISBN 978-3-9816764-8-8

Koehler S. A., Hilgenfeldt S., Stone H. A.: Foam drainage on the microscale: I. modeling flow through single plateau borders. Journal of colloid and interface science, 276(2):420–438, 2004.
Koehler S. A., Hilgenfeldt S., Stone H. A.: Liquid flow through aqueous foams: the node-dominated foam drainage equation. Physical review letters, 82(21):4232, 1999.
Lehmann E., Vontobel P., Wiezel L.. Properties of the radiography facility neutra at sinq and its potential for use as european reference facility. Nondestructive Testing and Evaluation, 16(2-6):191–202, 2001.
Marze S., Guillermic R.-M., Saint-Jalmes A.: Oscillatory rheology of aqueous foams: surfactant, liquid fraction, experimental protocol and aging effects. Soft Matter, 5(9):1937– 1946, 2009.
Neethling S. J.: Effect of simple shear on liquid drainage within foams. Physical Review E, 73(6): 061408, jun 2006. doi: 10.1103/physreve.73.061408.
Princen H. M.: Gravitational syneresis in foams and concentrated emulsions. Journal of colloid and interface science, 134(1):188–197, 1990.
Safouane M., Durand M., Saint-Jalmes A., Langevin D., Bergeron V.: Aqueous foam drainage. role of the rheology of the foaming fluid. Le Journal de Physique IV, 11(PR6):Pr6–275–Pr6–280, oct 2001. doi: 10.1051/jp4:2001633.
Saint-Jalmes A.: Physical chemistry in foam drainage and coarsening. Soft Matter, 2(10): 836–849, 2006.
Verbist G., Weaire D., Kraynik A. M.: The foam drainage equation. Journal of Physics: Condensed Matter, 8(21):3715, 1996.

GALA e.V., Karlsruhe, Germany, ISBN 978-3-9816764-8-8